Near-Infrared Light-Responsive Semiconductor Polymer Composite Hydrogels: Toward Spatial/Temporal Controlled Release via Photothermal "Sponge" Effect

*Yingjie Wu, Kai Wang, Shuo Huang, Cangjie Yang and Mingfeng Wang**

School of Chemical and Biomedical Engineering, Nanyang Technological University, 62 Nanyang Drive, 637459, Singapore

ABSTRACT: Near-infrared (NIR) light-responsive hydrogels are important for biomedical applications such as remotely controlled release, but the NIR agents previously used were largely limited to heavy-metal inorganic materials such as gold nanoparticles. In this article, we report a new type of NIR photothermal responsive hydrogels, which could undergo structural changes in response to NIR light for biomedical applications in drug delivery and controlled release. The hydrogels synthesized by integrating a narrow bandgap semiconductor polymer poly(diketopyrrolopyrrole-*alt*-3,4-ethylenedioxythiophene) (PDPPEDOT) with polymerization of *N*-isopropylacrylamide (NIPAM) show rapid and reversible mechanical shrinkage upon NIR light irradiation and can serve as carriers for anticancer drug loading and spatial/temporal control of drug release. These stimuli-responsive hydrogels, which can be prepared into different sizes

and shapes, integrate photothermal property and hydrogel characteristics, can provide on-demand, repeated, remotely controlled drug delivery for biomedical applications such as cancer treatment.

KEYWORDS: PNIPAM, hydrogel, semiconducting polymer, photothermal effect, drug delivery, controlled release

INTRODUCTION

Hydrogels have attracted great interest in biomedical applications, because of their excellent properties such as biocompatibility, high compressibility and water content, reversible volume-change, tunable physical and chemical properties and other functions such as stimuli-sensitivity.[1-3] One remarkable application of hydrogels is for drug delivery in which hydrogels can simply mix drugs in the solution state and achieve drug encapsulation, and directly deliver the payload to targeted sites.[4,5] The disadvantages of traditional hydrogels in terms of weak mechanical properties, uncontrollable release and slow switching kinetics have limited their practical applications. There have been more and more interests in developing a new generation of stimuli-responsive hydrogels.[6-8]

To overcome the aforementioned limitations, the new intelligent hydrogels can change the volume, permeability and other properties in response to the stimulation of surrounding conditions including temperature,[9,10] pH value,[11-13] light,[14] ultrasound,[15] electric and magnetic fields.[16,17] Among the stimuli-responsive hydrogels, some efforts have been devoted to preparing near-infrared (NIR)-triggered thermally responsive hydrogels to achieve on-demand controllable drug release profile, because NIR light stimulus can be easily and remotely controlled with

adjustable intensity and wavelength, as well as ease of spatial/temporal control, as compared with other stimuli. Hayward and co-workers reported on-demand reconfigurable buckling of a PNIPAM hydrogel film embedded with gold nanoparticles (Au NPs) by patterned photothermal deswelling.[18] Lin and co-workers reported a PNIPAM hydrogel embedded with carbon nanotubes, in which carbon nanotubes acted as a molecular heater through photothermal conversion effect to raise the local temperature of the hydrogel.[19] Langer, Kohane and coworkers fabricated a thermoresponsive PNIPAM hydrogel embedded with hollow gold nanoshells and implanted in diabetic rats. These hydrogels enabled controllable release of aspart, a fast-acting analogue of insulin, upon NIR-light irradiation.

Nevertheless, some limitations still exist in the previously reported photothermal responsive systems, such as incomplete reversibility, slow switching kinetics, use of ultraviolet light and high cytotoxicity of heavy metals from the inorganic NIR light-absorbing agents. As a consequence, new types of photothermal agents with desirable biocompatibility and biodegradability are needed for biomedical applications.[20] For instance, Zhang and co-workers incorporated polydopamine nanoparticles (PDA-NPs) into PNIPAM networks, resulting in a triply responsive hydrogel of PDA-NPs/PNIPAM with properties of pulsatile drug release, NIR-driven actuation, and NIR-assisted healing.[21] Nevertheless, the poorly defined chemistry involved in the synthesis of PDA often results in NPs with chemical structures that are difficult to identify, nontunable optical properties without well-defined absorption bands, and particle sizes not easy to control. Such shortcomings might limit the scope of the applications of PDA NPs for photothermal therapy and controlled release.

Semiconducting polymers are a new class of optical soft materials with tunable optical, electronic and mechanical properties that are promising for applications such as photovoltaic and

light emitting devices as well as imaging of biomolecules, cells and tissues.[22-26] Compared to inorganic materials, semiconducting polymers are expected to have better biocompatibility/biodegradability and no heavy-metal-ion induced toxicity to living organisms.[27-30] Compared to polymdopamine-based photothermal agents aforementioned, semiconducting polymers (often appended with alkyl side chains to improve the solubility and processability) show advantages such as their well-defined chemical structures and molecular weights, precisely tunable optical properties and high light-absorption coefficiency, and good solution-processability to achieve colloidal nanoparticles with controllable sizes and shapes.[31] Due to the excellent photo-thermal conversion efficiency and good biocompatibility, the semiconducting polymers as organic alternatives of gold nanoparticles,[32] gold nanorods,[33] and gold nanoshells[10,34] can be combined with thermally responsive hydrogels as photon antenna to realize photothermal transformation. These semiconducting polymers can absorb NIR light and convert light into heat, raise the local temperature of the gel and therefore control the release behavior of the hybrid hydrogel.[35] Semiconducting polymers have been widely used in biomedical applications such as optical imaging for disease diagnosis, controlled release and tumor treatment.[36,37] Our previous work reported some new photothermal agents based on π-conjugated small molecules with strong absorption of NIR light. The prepared benzo[1,2-c;4,5-c']bis[1,2,5]thiadiazole-4,7-bis(5-(2-ethylhexyl)thiophene) (BBTEHT)[23] NPs and benzo[1,2-c;4,5-c']bis[1,2,5]thiadiazole-4,7-bis(9,9-dioctyl-9H-fluoren-2-yl)thiophene (BBT-2FT)[36] NPs showed higher photothermal conversion efficacy and improved photostability compared to that of commercial gold (Au) nanorods. The BBT-2FT NPs even can be used for dual-modal photoacoustic imaging and photothermal therapy.[23,38] Nevertheless, these NIR-light absorbing organic NPs have not been incorporated into stimuli-responsive hydrogels for controlled release.

Diketopyrrolopyrrole (DPP), especially thiophene-flanked DPP, with high coplanar nature, was an important building block to construct conjugated polymers with narrow bandgaps. DPP-based conjugated polymers have been widely used in high-performance organic electronic devices, such as organic field effect transistors (OFETs)[39-45] and organic photovoltaics (OPVs)[46,47], as well as for photoacoustic imaging.[48]

Here we report a new application of a DPP-based narrow bandgap polymer (denoted as PDPPEDOT, with its chemical structure shown in Figure 1A) for remotely NIR-light controlled release. PDPPEDOT showing strong photothermal effect upon absorbing NIR light in the form of either colloidal nanoparticles (NPs) or thin films was integrated with thermal responsive hydrogels consisting of poly(N-isopropylacrylamide) (PNIPAM). The resulting composite hydrogels uploaded with hydrophilic drugs mechanically shrink upon irradiation of 808-nm NIR laser light and induce the drug release. Such mechanical shrinking/swelling of the composite hydrogels is reversible upon many cycles of ON/OFF NIR light irradiation. The NIR-light controllable drug release has been demonstrated using doxorubicin (DOX) as an example of anticancer drugs. Furthermore, the structural characterization, in vitro cytotoxicity and drug release capacity of this system in cancer therapy were studied in detail.

Experimental Section

Materials *N*-isopropylacrylamide (NIPAM, purchased from SigmaAldrich) was purified by recrystallization. Methylene bisacrylamide (MBAm), ammonium persulfate (APS), N,N,N',N'-tetramethyl-ethylenediamine (TEMEDA), Pluronic 127 and tetrahydrofuran (THF) were all purchased from Sigma-Aldrich. poly(9,9-bis(3'-(N,N-dimethyl)-propyl-2,7-fluorene)-*alt*-2,7-(9,9-dioctylfluorene)) (PFN-P1) was from 1-Material Inc. All other chemicals used for synthesizing graphite oxide were of analytical grade and used without further treatment.

Dulbecco's Modified Eagle's Medium (DMEM), fetal bovine serum (FBS), penicillin/streptomycin mixture, phosphate buffered saline (PBS), Alexa Fluor® 633 phalloidin, TrypLE™ Express Enzyme (1×), DAPI (4',6-diamidino-2-phenylindole) and PrestoBlue cell viability reagent were purchased from Life Technologies (Singapore). Pure water (18.2 MΩ at 25 °C) from a Milli-Q Plus water purification system (Millipore) was used throughout the experiments.

Synthesis of PDPPEDOT via direct arylation polymerization. A 5 mL microwave tube with a magnetic stirrer bar was charged with mixture of $Pd_2(dba)_3{\cdot}CHCl_3$ (10.4 mg, 0.01 mmol), K_2CO_3 (82.8 mg, 0.60 mmol), P(*o*-MeOPh)$_3$ (7.0 mg, 0.02 mmol), PivOH (10.2mg, 0.10 mmol), 3,4-ethylenedioxythiophene (28.4 mg, 0.20 mmol), and 3,6-bis(5-bromothiophen-2-yl)-2,5-bis(2-ethylhexyl)-pyrrolo[3,4-*c*]pyrrole-1,4(2H,5H)-dione (DTDPP-Br) (136.5 mg, 0.20 mmol) and then placed in the glove box. *o*-Xylene (1 mL) was added into the mixture and the tube was capped with a septum before taking out of the glove box. The mixture was stirred at room temperature for 5 min and then placed in a pre-heated oil bath at 100 °C for 24 hours. After cooling to room temperature, the reaction mixture was poured into ice methanol. The resulting solid was filtered and subjected to Soxhlet extraction in methanol and hexane for the removal of low molecular weight materials and impurities. The remaining polymer was extracted with chloroform, precipitated again from ice methanol and dried under vacuum.

Preparation of photothermal PDPPEDOT nanoparticles. PDPPEDOT (1 mg) was dissolved in THF (1 mL) by bath sonication. The resulting solutions were filtered through a polyvinylidene fluoride (PVDF) syringe driven filter (0.22 μm) (Millipore). Then, a THF solution (1 mL) containing PDPPEDOT (0.25 mg/ mL) and Pluronic F127 (5 mg/mL) was used to prepare PDPPEDOT NPs by rapidly injecting the solution into deionized water (9 mL) under

continuous sonication with a bath sonicator (Branson 250). After sonication for additional 1 min, THF was evaporated at 65 °C under nitrogen atmosphere.

Preparation of photothermal PDPPEDOT film. Thin films of PDPPEDOT were prepared using a spin coating method. PDPPEDOT was dissolved in chloroform to reach a concentration of 10 mg/mL. The solution was spin coated on 2×2 cm glass substrates with speed of 5000 rpm. In order to enhance the adhesion of the hydrogel with PDPPEDOT film, we further spin-coated PFN-P1 (2 mg/mL in methanol) as a kind of more hydrophilic conjugated polymer on the PDPPEDOT film to enhance the surface-wetting properties in aqueous media.

Synthesis of PNIPAM hydrogel. The PNIPAM copolymer hydrogel was synthesized by free radical polymerization method. The PNIPAM copolymer hydrogel between the N-isopropylacrylamide (NIPAM) monomer and methylene bisacrylamide (MBAm) was prepared through the free radical solution polymerization using ammonium persulfate (APS) as an initiator. 148 mL of an aqueous solution of NIPAM (0.24 g/mL) mixed with 500 μg/mL of DOX, 19.4 mL of an aqueous solution of MBAm (0.02 g/mL) and 2.1 mL of deionized water were added sequentially. The solution was degassed, and 1 mL of N, N, N', N'-tetramethylethylenediamine and 2 mL of APS solution (0.1 g/mL) were added to initiate polymerization. This pre-gel mixture was injected onto the film of PDPPEDOT, placed in an airtight bottle, purged with nitrogen and allowed to polymerize for 1 h or longer.

Photothermal conversion efficiency of PDPPEDOT. NIR laser at 808 nm with intensity of 0, 0.8, 1.2, 1.6, 2 W/cm^2, respectively, was employed to illuminate the PDPPEDOT film or NPs in water. The temperature variation was detected by a thermoprobe. The temperature recording was done every five seconds. The photothermal conversion efficiency of PDPPEDOT was refered to the previous reported method.[38,49,50] PDPPEDOT dissolved in toluene with

concentration of 10 mg/mL. The photothermal conversion efficiency (η) was calculated by the equation described in Supporting Information and the results are shown in Figure S4.

Drug release behavior test. The composite systems were put into a small bottle with 5 mL deionized water. The hydrogel was irradiated from the upside by a continuous laser with an output wavelength of 808 nm. An aliquot of 50 μL of the solution was withdrawn every five minutes from laser on while equal amounts of water were injected into the bottle. Fluorescence detection of DOX release was test with excitation on 495 nm and absorption on 505 nm.

In vitro experiments. *Cell culture*: HeLa cells were regularly cultured in Dulbecco's modified Eagle's medium (DMEM) supplemented with 10% FBS and 1% penicillin/streptomycin at 37 ºC with 5% CO_2 in a humidified incubator.

In vitro cytoactive assays: The viabilities of HeLa cells were evaluated by applying a PrestoBlue assay. The polymer and hydrogel composite system were cut into right size and put into the 96-well plate. The equivalent amounts of hydrogel without polymer film/nanoparticle and only cell groups were also employed as control. About 1×10^5 cells per hole were cultivated in 96-well plate. The viabilities of cells under different laser intensity irradiation were statistics. In order to see the laser induced photothermal conversion effect, cells were cultured at 30 ºC with 5% CO_2 in a humidified incubator.

In vitro cell imaging by confocal laser scanning microscopy: Cells were fluorescently labeled according to our previously reported method,[51] and the details were described in Supporting Information. For photothermal drug release study, 1 mL of cell suspension with a cell density of ~1×10^6 cells per mL was inoculated on coverslips in a well plate incubated for 12 h in the incubator first. Then the face-up hydrogel supported on a glass substrate was incubated with the

cell culture media (Figure S10). After NIR laser irradiation for 20 min, the cells incubated for 2 and 12 h, respectively, at 30 ºC with 5% CO_2.

Characterization. Transmission electron microscopy (TEM) images were acquired with a TEM Carl Zeiss Libra 120 Plus operating at an acceleration voltage of 120 kV. UV-vis absorption spectra were recorded on a Varian Cary 4000 UV-vis spectrophotometer.

The morphological characterization of the hydrogel: The morphological structures of the hydrogels were observed by scanning electron microscopy (SEM, JSM6390LA) at 10 kV. The hydrogel samples were separately frozen in -80 °C refrigerator before and after laser irradiation respectively, followed by freeze-drying overnight. The dry samples were quickly fractured to expose their inner structures and coating with platinum using a sputter-coater for 120 s at 20 mA.

RESULTS AND DISCUSSION

Synthesis and characterization of the semiconducting polymer PDPPEDOT. The semiconducting polymer, denoted as PDPPEDOT, used in this study was synthesized via direct arylation polymerization (Figure S1) recently established in our laboratory.[52-59] This synthetic protocol does not involve pre-activation of the arene monomer using flammable (e.g. BuLi) and toxic (e.g. organo-tin agent) organometallic reagents, thus enabling facile synthesis of the target polymers in fewer synthetic steps compared to conventional Suzuki coupling and Stille coupling methods.[43,60] The chemical structure of the polymer PDPPEDOT is shown in Figure 1A. The number-average molecular weight (M_n) and polydispersity index (PDI) of the obtained polymer were measured with gel permeation chromatography (GPC). After the direct arylation polymerization, the resulting PDPPEDOT showed monomodal GPC peaks by both RI and UV-Vis detectors (Figure S2), giving M_n around 12600 g mol^{-1} and a PDI of 2.4. The ^{1}H-NMR spectrum of PDPPEDOT (Figure S3) shows two broad peaks in the aromatic range at 9.1 (H_a)

and 7.9 (H_b) ppm, respectively, which could be attributed to the protons in the thiophene rings from DTDPP unit in the conjugated polymer backbone. Protons in the EDOT unit (H_d) and DPP side chain (H_c) were found around 4.0 ppm with other protons located in the aliphatic range from 0.8 to 2.0 ppm. The UV-vis–NIR absorption spectra of PDPPEDOT in chloroform showed the maximum absorption peak at 765 nm (Figure 1B).

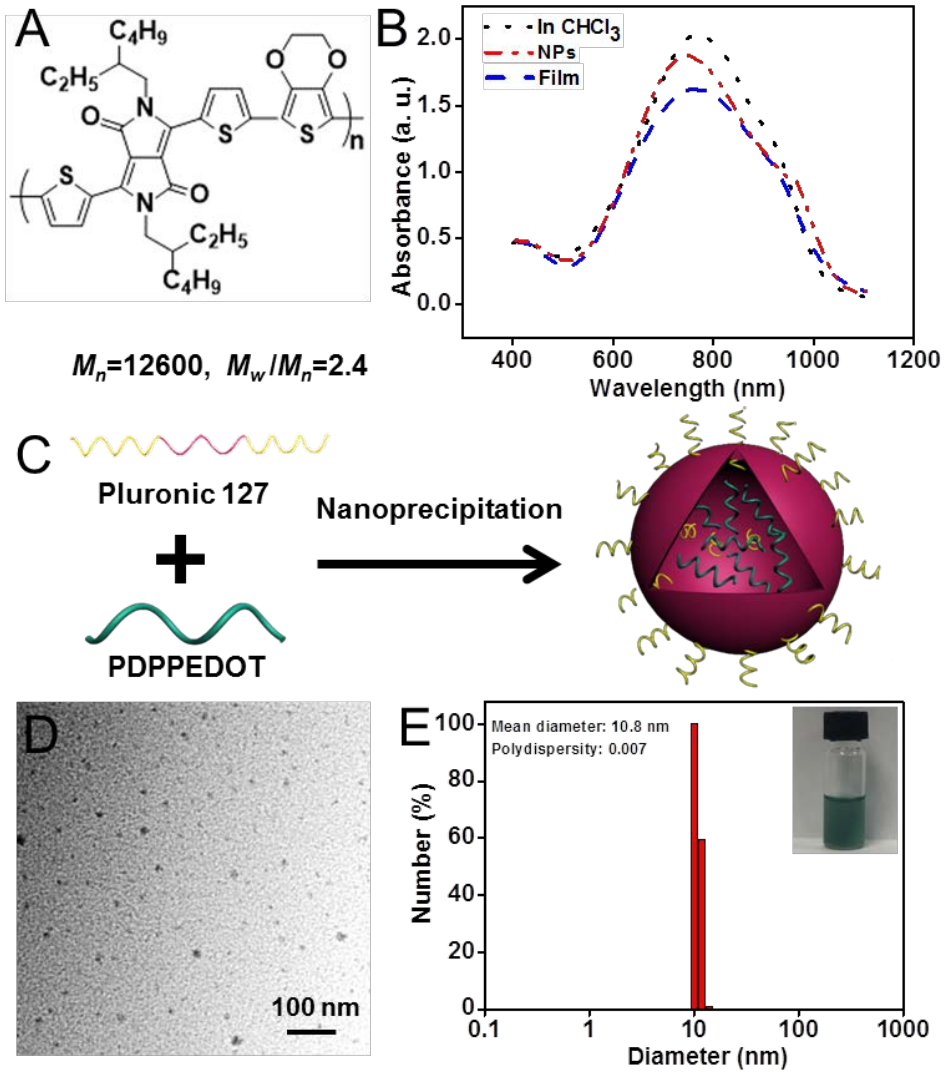

Figure 1 (A) Chemical structure of semiconducting polymer PDPPEDOT. (B) UV-vis absorption spectra of PDPPEDOT polymer in $CHCl_3$, PDPPEDOT NPs in water and PDPPEDOT polymer film. (C) Schematic illustration of preparation of PDPPEDOT NPs. (D, E) TEM image and DLS histogram of PDPPEDOT NPs.

PDPPEDOT is essentially hydrophobic. In order to render it dispersible into aqueous media, we prepared the colloidal nanoparticles (NPs) of PDPPEDOT via a nanoprecipitation approach by employing amphiphilic copolymer Pluronic F127 as the stabilizer to encapsulate the PDPPEDOT polymers into the hydrophobic core of NPs (Figure 1C).[23] The morphology and size of the prepared PDPPEDOT NPs were characterized by transmission electron microscopy (TEM) and dynamic light scattering (DLS). The TEM image indicates that PDPPEDOT NPs had a uniform spherical morphology with an average diameter around 10 nm (Figure 1D). The DLS histogram (Figure 1E) of the NPs gave a hydrodynamic diameter around 11 ± 2 nm in aqueous solution, which agrees well with the TEM result (10 ± 2 nm). UV-vis absorption spectra of PDPPEDOT NPs in aqueous medium showed the maximum absorption peak at 745 nm, while the maximal absorption of PDPPEDOT spin-coating film was at 755 nm (Figure 1B). The minor change of the optical absorption of PDPPEDOT in colloidal NPs and in thin films versus in chloroform ($CHCl_3$) could be attributed to the intermolecular aggregation of conjugated polymer chains in the former cases.

Photothermal conversion of PDPPEDOT film and nanoparticles. The photothermal property of PDPPEDOT was first examined in $CHCl_3$ in which the polymer is well dissolved. The photothermal conversion efficiency (η) upon laser irradiation at 808 nm was calculated to be 27%, which is higher than that of gold NPs (η= 3.4-9.9%)[50] or nanorods (η= 17-22%),[49,61] and similar to other reported semiconductor polymers (η = 30%).[61] The calculation process was shown in section of Experimental Method and Figure S4. The photothermal properties of PDPPEDOT film and NPs were studied and compared under irradiation of different laser powers. The PDPPEDOT NPs were dispersed in 3 mL of water (Figure S5A) and the PDPPEDOT film precast on a glass substrate was also submerged in 3 mL of water (Figure S5B), both of which

were subjected to light irradiation from a 808-nm NIR laser with different light intensities. The temperature variation of water caused by the photothermal effect of polymer at different time intervals was monitored using a thermocouple probe.

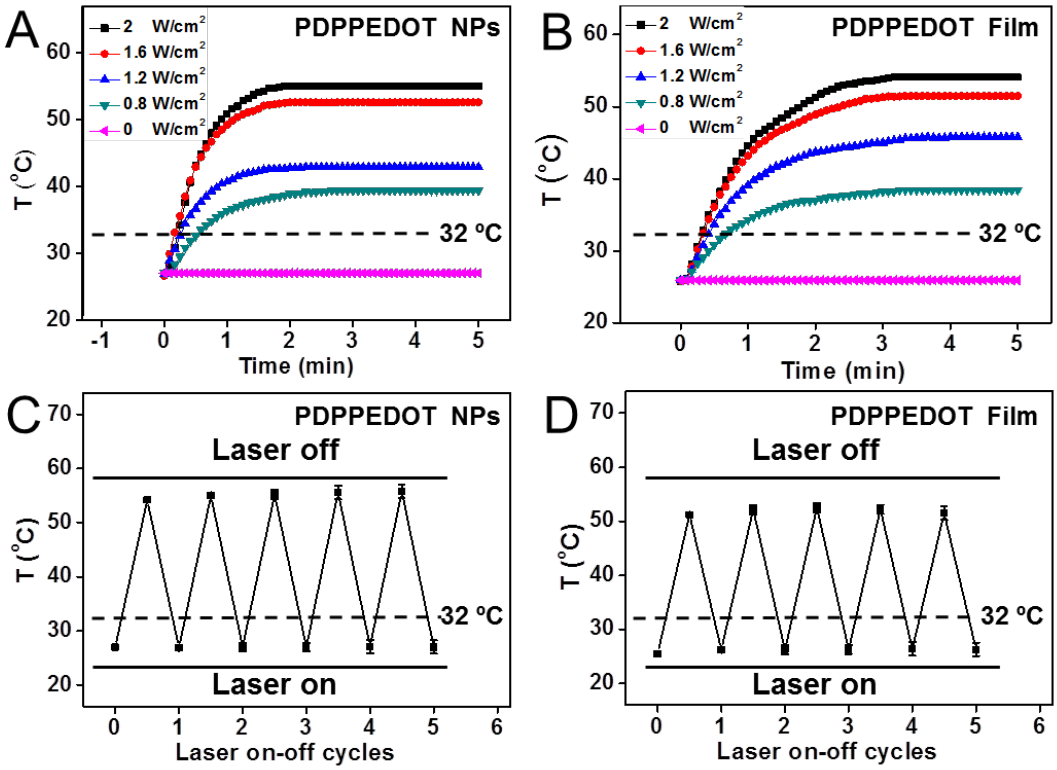

Figure 2 Photothermal conversion behavior of PDPPEDOT colloidal NPs in water (A, C) and spin-cast films on glass substrates (B, D) under 808-nm laser irradiation at a power of 1.6 W/cm^2. In C and D each cycle exposure to NIR light was kept for 5 min.

Under continuous laser irradiation at 808 nm over the range of 0.8-2 W/cm^2, PDPPEDOT films and NPs showed gradual increase of the solution temperature, whereas PDPPEDOT films and NPs without laser irradiation showed negligible change of the temperature (Figure 2A,B). Upon the NIR irradiation, the temperature raised quickly over the hydrogel's lower critical solution temperature (LCST) of PNIPAM at 32 °C. Even at a low intensity of NIR irradiation (0.8 W/cm^2), the temperature of PDPPEDOT film and NPs can increase from room temperature (25 °C) to 38 °C over one minute. Moreover, the intensity of NIR irradiation can also influence

the temperature variation. A higher temperature can be achieved by increasing the power of the NIR irradiation. The maximum photothermal temperature of the PDPPEDOT film could reach 54 °C, while the aqueous dispersion of PDPPEDOT NPs could reach 56 °C under the NIR irradiation with a power of 2 W/cm^2. By repeating the on/off cycle of the NIR laser irradiation, the temperature response can be reversible (Figure 2 C and D). This result indicates that such NIR light-induced temperature rise of polymer is not only significant and rapid but also reversible.

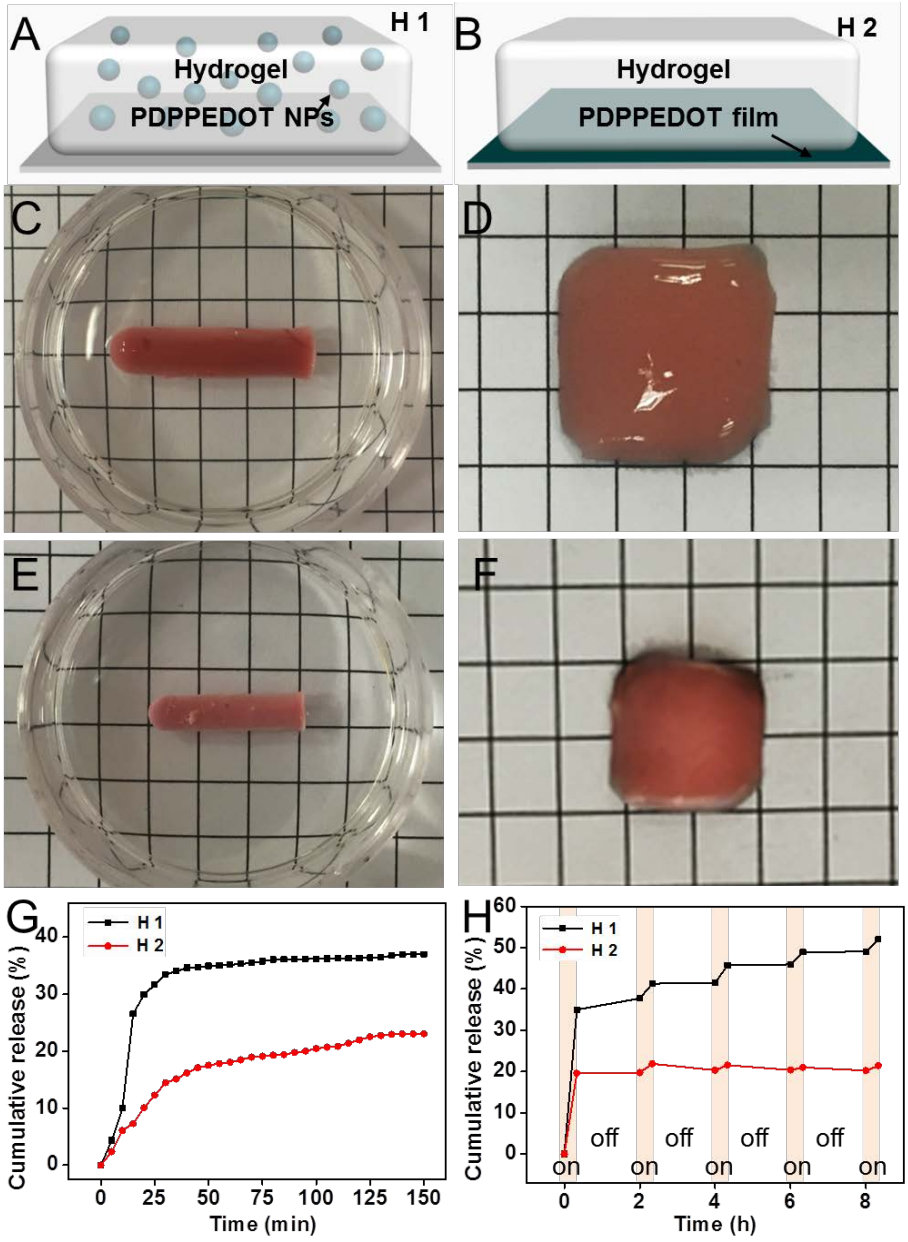

Figure 3 (A, B) Schematic illustrations of **H1** (A) and **H2** (B) hydrogels. Digital photographs of photothermal response of DOX-loaded **H1** hydrogel with a 3D cylindrical shape (C, E) and **H2** hydrogel film (D, F) before (C, D) and after (E, F) 808-nm laser irradiation at a power of 1.6 W/cm^2 for 5 min. (G, H) The in vitro drug release of **H1** and **H2** hydrogel under 1.6 W/cm^2 laser irradiation (808 nm). The grid size of the background in (C-F) was 0.5×0.5 cm^2.

Preparation and characterization of PDPPEDOT/PNIPAM composite hydrogels. The PNIPAM copolymer hydrogel was synthesized by a method of free radical polymerization in the

presence of N', N'-methylene bisacrylamide (MBAm) as the crosslinker. More details of the hydrogel synthesis are described in the Experimental Section. PDPPEDOT was selected as the NIR photothermal agent because of its excellent photothermal conversion property as demonstrated in Figure 2. Here PDPPEDOT was integrated with the PNIPAM hydrogels described above through two different strategies as shown in Figure 3A-B. The composite hydrogel with PDPPEDOT NPs with an average diameter of 10 nm dispersed into PNIPAM networks was denoted **H1**, while the PNIPAM hydrogel standing on the top of spin-cast PDPPEDOT film was denoted as **H2**. In **H1** hydrogel (Figure 3A), PDPPEDOT NPs were premixed with the hydrogel precursor, followed by the polymerization that resulted in a composite hydrogel with PDPPEDOT NPs homogeneously dispersed in the hydrogel matrices. In **H2** hydrogel (Figure 3B), the hydrogel precursor was cast on a pre-spin-cast PDPPEDOT film supported on a glass substrate. The following polymerization under the reaction condition described above resulted in a PNIPAM hydrogel standing on the top of PDPPEDOT films. In both **H1** and **H2** hydrogels, the semiconducting polymer PDPPEDOT acts as a molecular photothermal agent to induce the hydrophilic-to-hydrophobic transition of PNIPAM matrices once the temperature is increased above the lowest critical solution temperature (LCST, 32 ^{o}C) of PNIPAM.[62]

The mechanical properties of the PNIPAM hydrogels are related to the concentration of the crosslinker, MBAm, added in the polymerization mixture. Figure S6A shows the stress-strain curves obtained by compression test. At C_{MBAm}= 0.01 g/mL, the stress is obviously lower than that of at 0.03 g/mL, which was expected as the lower concentration of crosslinker led to lower crosslinking density and thus weaker mechanical strength.

To investigate the influence of the mechanical property to drug release behavior, we compared the cumulative drug release of hydrogels with different concentrations of crosslinker (MBAm). We prepared hydrogels with crosslinker concentration of 0.01, 0.02, 0.03 g/mL, respectively. As illustrated in Figure S6B, it was observed that 26% of the drug (i.e. DOX) was released from hydrogel with 0.01 g/mL MBAm after 200 min irradiation under 1.6 W/cm^2 NIR laser light, while 19% of drug release from hydrogel with 0.03 g/mL MBAm under the same irradiation condition. These results indicated that lower concentrations of the crosslinker led to lower compressive strength of the hydrogel and thus more drug release (Figure S6B). Moreover, if the concentration of the crosslinker was lower than 0.01 g/mL, the pNIPAM could not form solid hydrogels. In order to maintain both good compression strength and drug release ability, we chose MBAm with a concentration of 0.01 g/mL for the following study.

Moreover, a model red-fluorescent anticancer drug doxorubicin (DOX) was loaded into the hydrogel by mixing a hydrophilic form of acidified DOX (denoted as DOX•HCl) with NIPAM monomers in the presence of crosslinker and initiator. The following polymerization at room temperature under inert atmosphere resulted in the PDPPEDOT/DOX/PNIPAM ternary composite hydrogel. NIR light at a wavelength of 808 nm was applied as a remotely controlled switch to trigger hydrogel shrinkage through photothermal conversion effect of PDPPEDOT.

To investigate the NIR-light stimulated response of polymer composite hydrogel, **H1** hydrogel with a 3D cylindrical shape was exposed under the NIR light at a power of 1.6 W/cm^2 (Figure 3C, E). The 3D PDPPEDOT/DOX/PNIPAM hydrogel exhibited obvious contraction and the color became lighter after 20 min of NIR laser irradiation. The shrinking extent of the hydrogel reached 40%. We speculate that PDPPEDOT nanoparticles in the interior composite generated a large amount of heat in the hydrogel, which leads to fast volume shrinkage that squeezes out of

encapsulated DOX through a “sponge” effect. Such NIR photo-responsive shrinkage of the composite hydrogel was also observed in another four hydrogels with different 3D shapes (Figure S7). Video S1 (speeded up to 30 times) displayed the NIR photo-responsive process of a **H1** hydrogel of 3D round disk shape. These stimuli-responsive hydrogels with reconfigurable volume and shape have many potential applications in multiple fields, such as scaffolds for tissue engineering, smart switch of chemical reactions, drug carriers, bioseparation, as well as artificial “muscles” and soft biomimetic machines. In comparison, the blank PNIPAM hydrogel in the absence of PDPPEDOT did not show any mechanical response upon 808-nm laser irradiation (Figure S8).

To verify the thermal shrinkage behavior of hydrogel, we characterized the cross section morphologies of the lyophilized hydrogel samples using scanning electron microscopy (SEM) to investigate the morphological characteristics of the hydrogels before or after laser irradiation. Hydrogel samples were quickly frozen in -80 °C refrigerator and freeze-dried. The lyophilized hydrogel samples were fractured to expose the cross sections. Figure S9 show the microstructures of freeze-dried 3D hydrogel samples. The pore size of the hydrogel before laser irradiation was obviously larger than that after laser irradiation. The diameter of holes before laser irradiation was more than 20 μm, and after laser irradiation the diameter changed into less than 5 μm. Such differences in pore structures are resulted from the hydrogel shrinking upon NIR laser irradiation. As a result, the drug release is directly affected by the mechanical contraction of the hydrogel, while the contractility is depending on the temperature variation from the photothermal effect.

We also carried out the control experiments and examined the photoresponsive behavior of PNIPAM hydrogels (with and without DOX, respectively) in the absence of PDPPEDOT. The

results are presented in Figure S8. There were neither significant mechanical response nor drug (DOX) release before and after the 808 nm laser irradiation. These results indicate that the photothermal agent of PDPPEDOT NPs plays an essential in the hydrogels to induce the NIR-light responsive mechanical shrinkage and the controlled drug release.

NIR triggered drug release of PDPPEDOT/PNIPAM composite hydrogels. The drug release ability of PDPPEDOT combined PNIPAM hydrogel was evaluated using both **H1** and **H2** hydrogels with a dimension of 20 × 20 × 2 mm^3 (Figure 3A). Each piece encapsulated 74 μg of DOX inside the hydrogel. The uniform polymer film adhered tightly to the hydrogel. Their mechanical shrinking behaviors as well as drug release properties are shown in Figure 3D, F and Figure S10.

The **H1** hydrogels were exposed to an 808-nm laser beam at 1.6 W/cm^2 for 20 min. Once the NIR light is turned on, PDPPEDOT absorbs NIR light and converts it into heat. As a result, the hydrogel mechanically shrunk, accompanied by DOX release in responding to the temperature rise. When the NIR laser was turned off, the hydrogel cooled down, re-adsorbed water and returned to its swelling state. The hydrogel slowly recovered to the original volume within 2 h. Under the laser irradiation again, the hydrogel re-contracted and recovered again when the laser was turned off (Figure S10 A). This process can be repeated more than 10 cycles without any hydrogel fatigue. Such reversible contracting response was also observed in **H2** hydrogel (Figure S10 B). In particular, the hydrogel became a little transparency and swollen after being soaked in aqueous solution for the first time. After sufficient swelling and absorption of water, the hydrogel recovered to its original swelling state after each NIR irradiation cycle.

Before the NIR laser irradiation, each piece of hydrogel was encapsulated with 74 μg of DOX. The in vitro release of DOX from **H2** hydrogel after NIR irradiation was quantified according to

the fluorescence intensity of DOX. Upon the NIR irradiation, the temperature instantly raised. Moreover, a higher release can be achieved by increasing the power of the NIR irradiation. As illustrated in Figure S10 C, 28% of the drug was released from the hydrogel after 200 min irradiation under 1.6 W/cm^2 NIR light (808 nm). While the control experiment showed that the drug release rate remained at a relative low level without NIR laser irradiation. Only a small quantity no more than 5% of DOX was leached out within 200 min, which is much lower than the NIR-triggered process. The NIR-triggered drug release was attributed to the hydrogel shrinking. Therefore, the drug release is minimal in the "NIR off" state and can be accelerated significantly upon NIR laser irradiation.

Figure 3G shows that the drug release from **H1** hydrogel was much faster than that from **H2** hydrogel under the same NIR irradiation with a power of 1.6 W/cm^2. Such difference is probably due to the uniform distribution of PDPPEDOT NPs in **H1** hydrogel which enables better heat transfer from PDPPEDOT to PNIPAM matrices. As a result, the drug release is directly affected by the mechanical contraction of hydrogel by the stimulation of NIR light irradiation, while the extent of the mechanical shrinkage is dependent on the temperature variation by the photothermal effect.

In order to improve the extent of the drug release, both **H1** and **H2** hydrogels were subjected to multiple cycles of "ON/OFF" laser irradiation to induce the reversible shrinking/swelling process of the hydrogels (Figure 3H). Within 20 min after the first NIR laser irradiation at the power of 1.6 W/cm^2, the cumulative amount of DOX release significantly increased to 36% and 19% in **H1** and **H2** hydrogels, respectively. Once the NIR laser was switched off, the release was reduced over the next 2 h. Although **H1** hydrogel still showed a minor release based on the drug diffusion before recovered to its swelling state, the hydrogel network provided a large hindrance

for DOX diffusion that restrains the drug release when the laser was turned off. When the NIR laser was switched on for the next 20 min, there was another burst of drug release. Although the hydrogel can be recontracted and recovered in **H2** system, further drug release was not obvious. Such difference of the release behavior between **H1** and **H2** hydrogels could be attributed to the fact that the heat conduction in **H2** hydrogel is not so good as in **H1** hydrogel, as discussed earlier. Thus, the sustained release of drugs can be achieved by repeatedly switching on/off NIR laser. A cumulative release of 54% DOX of **H1** hydrogel was achieved after five cycles of "ON/OFF" laser irradiation.

In addition, we have employed UV-vis spectroscopy to detect the potential leakage of PDPPEDOT NPs from **H1** hydrogel. We cut the PNIPAM hydrogel loaded with PDPPEDOT NPs in two halfs with equal weight. One half was immerged into water and subjected to three cycles of "ON/OFF" laser (808 nm) irradiation to induce the reversible shrinking/swelling process, while the other half was kept intact. The water in the two vials containing the hydrogels remained colorless after the laser irradiation. Then PDPPEDOT remained in hydrogels were collected by soaking the hydrogels in THF. The results of UV-vis absorption spectra (Figure S11, revised Supporting Information) demonstrated that there was little leakage of the PDPPEDOT NPs from the matrices of PNIPAM hydrogel.

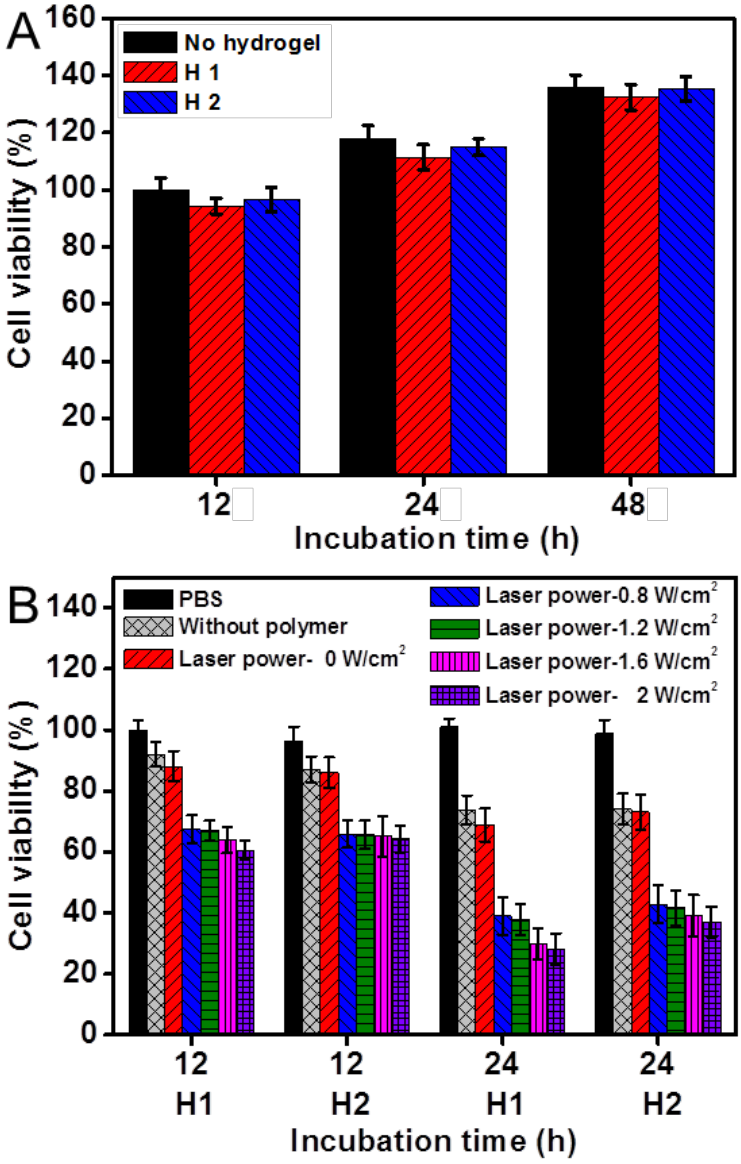

Figure 4 Cell viability of HeLa cells tested by PrestoBlue assay. (A) Cytotoxicity assay after co-culture with **H1** and **H2** hydrogel over 12, 24 and 48 h. (B) Cell viability after treatment with DOX-encapsulated hydrogels under 0-2 W/cm^2 laser irradiation (808 nm).

In vitro cell studies of PDPPEDOT composite hydrogels. The biocompatibility of **H1** and **H2** hydrogels without any encapsulated drugs was examined using Presto blue assays. Results are shown in Figure 4A. The cells were able to proliferate well in the presence of **H1** and **H2** hydrogel, with proliferation similar to the negative control (no presence of the hydrogel) for 12,

24 and 48 h under the same experimental conditions. We also compared the cell viability in the presence of non-DOX-loaded **H1** and **H2** hydrogels over 12 and 24 h, respectively, with or without 808-nm laser irradiation. The results shown in Figure S12 indicate comparable cell viability in these experiments. The good biocompatibility of the present composite hydrogel systems even under the laser irradiation is presumably attributed to the conversion of the photothermal energy into the mechanical shrinkage (work) of the PNIPAM hydrogels, thus no significant hyperthermia effect on the cells in the cell-culture media outside the hydrogels.

Based on the in vitro drug release behavior shown in Figure 3, we expected that this hydrogel system could effectively release drug for cancer therapy. HeLa cells were cultured with the hydrogel substrate containing 74 μg of DOX. The schematic illustration of in vitro cell studies with **H1**/**H2** PDPPEDOT composite hydrogels is shown in Figure S13. Cells cultured with the hydrogel under laser irradiation showed lower cell viability compared to the control group without laser irradiation. The hydrogel killed more than 30% HeLa cells after incubated for 12 h and 60% HeLa cells were killed after 24 h incubation (Figure 4B). The cell death can be primarily attributed to the release of DOX triggered by the shrinkage of the hydrogels upon laser irradiation.

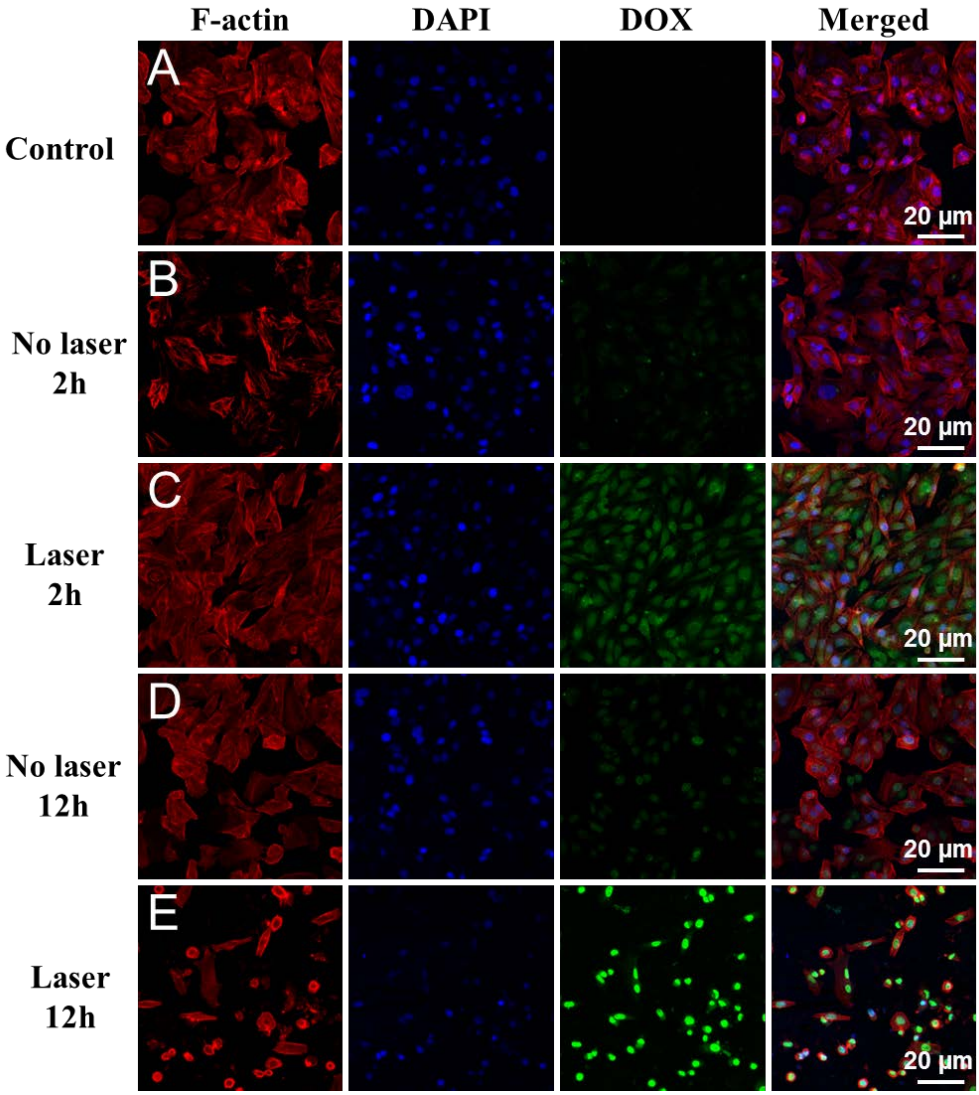

Figure 5. Confocal fluorescence images of HeLa cells incubated with **H1** hydrogel under different laser irradiation condition. (A) Initial state of the cell. (B-E) HeLa cells treatment with **H1** hydrogel after 20 min laser irradiation and continue incubated for 2 and 12 h respectively. Red: F-actin stained cytomembrane, blue: DAPI stained nucleus, green: pseudo label of DOX localization, right: merge images.

Furthermore, the process of DOX release from hydrogel and uptake by HeLa cells were studied using confocal laser scanning microscopy (CLSM). The cell nucleus was stained by DAPI while cell membrane was stained by F-actin. Figure 5 shows the CLSM images of HeLa cells continuously incubated with **H1** hydrogel for 2 h and 12 h, respectively, after 20-minute

laser (808 nm) irradiation. Before laser irradiation, the image shows that the cells with normal morphology and little fluorescence of DOX were observed inside the cell. After NIR laser irradiation, strong fluorescence from the excited DOX localized homogeneously in the cytoplasm region of HeLa cell was clearly observed (Figure 5C) after 2-h incubation with the irradiated hydrogels. These results indicate that the DOX was successfully released from the hydrogel and internalized by the tumor cells. After 12 h incubation with the NIR-laser irradiated hydrogel, one can see that the free DOX was mainly localized at the nucleus of the cancer cells, accompanied with morphological change of the cellular membrane and detachment of cells from the substrate, as shown in Figure 5E. From these images, we can clearly see the shrinkage of cell membranes in these cells in Figure 5E compared with the controls in Figure 5A. These results are consistent with the obvious cytotoxicity observed over 12 h incubation after NIR laser irradiation shown in Figure 4B. In contrast, cell incubated with the same hydrogel for 12 h without laser irradiation resulted in only relatively weak fluorescence in cell nuclei (Figure 5D). This phenomenon was also observed in the cells incubated with **H2** hydrogels (Figure S14). Considering the results mentioned above, we conclude that after NIR-induced drug release, DOX can enter the cytoplasm of HeLa cells within 2 h and deliver DOX moieties into the nuclei within 12 h.

CONCLUSION

In summary, we have reported a novel NIR light-responsive composite hydrogel consisting of a narrow-bandgap semiconducting polymer (PDPPEDOT) and PNIPAM. The hydrogel shrinkage and drug release behavior of these hydrogel systems under NIR laser irradiation were successfully demonstrated. When the PDPPEDOT/PNIPAM composite hydrogels subjected to NIR laser irradiation, the temperature increase of the system led to the shrinkage of the hydrogel and thereby accelerating the release of the loaded drug molecules. In contrast to the conventional

hydrogel, these composite hydrogels can provide on-demand, repeatable, remotely controlled drug delivery over extended periods. Such a remote triggering drug-release system provides the possibility of flexible spatial/temporal control regarding the desired location, dose magnitude, and timing. Therefore, we believe that these NIR-light responsive hydrogels are promising as remotely controllable drug delivery systems for a variety of biomedical applications. For example, other therapeutic drugs may also ben encapsulated using the present approach. The light absorption wavelength in NIR region could be tuned using a variety of narrow bandgap π-conjugated small molecules and polymers. These photothermal responsive hydrogels could be used, for example, as implants for spatially/temporally controlled release or as patches for skin therapy.

ASSOCIATED CONTENT

Supporting Information.

The Supporting Information is available free of charge on the ACS Publications website at DOI: ×××.

Schematic of PDPPEDOT synthesis, GPC trace, the chemical structure and 1H-NMR spectra of PDPPEDOT; stress-strain curves and drug release curves of **H1** hydrogels with different crosslinking densities; photothermo response of **H1** hydrogel with different geometrical shapes and wafer shaped PNIPAM blank hydrogel without NIR-light; photographs of reversible contracting response of **H2** hydrogel; Schematic of in vitro cell studies with **H1**/**H2** PDPPEDOT composite hydrogels; confocal fluorescence images of HeLa cells incubated with hydrogel **H2**.

Movie of the NIR photo-responsive process of a **H1** hydrogel of 3D round disk shape, the video speeded up to 30 times (AVI).

AUTHOR INFORMATION

Corresponding Author

*E-mail：mfwang@ntu.edu.sg.

Notes

The authors declare no competing financial interest.

ACKNOWLEDGMENTS

We are grateful to the funding support by a start-up grant (M4080992.120) of Nanyang Assistant Professorship from Nanyang Technological University, AcRF Tier 1(M4011061.120, RG49/12) and AcRF Tier 2 (M4020172.120, ARC 36/13) from the Ministry of Education, Singapore.

REFERENCES

(1) Sun, J. Y.; Zhao, X. H.; Illeperuma, W. R.; Chaudhuri, O.; Oh, K. H.; Mooney, D. J.; Vlassak, J. J.; Suo, Z. G. Highly Stretchable and Tough Hydrogels. *Nature* **2012**, *489*, 133-136.

(2) Imran, A. B.; Esaki, K.; Gotoh, H.; Seki, T.; Ito, K.; Sakai, Y.; Takeoka, Y. Extremely Stretchable Thermosensitive Hydrogels by Introducing Slide-Ring Polyrotaxane Cross-Linkers and Ionic Groups into the Polymer Network. *Nat. commun.* **2014**, *5*, 5124.

(3) Balakrishnan, B.; Banerjee, R. Biopolymer-Based Hydrogels for Cartilage Tissue Engineering. *Chem. Rev.* **2011**, *111*, 4453-4474.

(4) Wei, H.; Cheng, S. X.; Zhang, X. Z.; Zhuo, R. X. Thermo-Sensitive Polymeric Micelles Based on Poly (N-isopropylacrylamide) as Drug Carriers. *Prog. Polym. Sci.* **2009**, *34*, 893-910.

(5) Wang, Y. J.; Chen, L. J.; Tan, L. W.; Zhao, Q.; Luo, F.; Wei, Y. Q.; Qian, Z. Y. PEG-PCL Based Micelle Hydrogels as Oral Docetaxel Delivery Systems for Breast Cancer Therapy. *Biomaterials* **2014**, *35*, 6972-6985.

(6) Kim, Y. S.; Liu, M.; Ishida, Y.; Ebina, Y.; Osada, M.; Sasaki, T.; Hikima, T.; Takata, M.; Aida, T. Thermoresponsive Actuation Enabled by Permittivity Switching in an Electrostatically Anisotropic Hydrogel. *Nat. Mater.* **2015**, *14*, 1002-1007.

(7) Tian, Z. C.; Chen, C.; Allcock, H. R. Injectable and Biodegradable Supramolecular Hydrogels by Inclusion Complexation Between Poly (organophosphazenes) and α-cyclodextrin. *Macromolecules* **2013**, *46*, 2715-2724.

(8) Shi, K.; Liu, Z.; Wei, Y. Y.; Wang, W.; Ju, X. J.; Xie, R.; Chu, L. Y. Near-Infrared Light-Responsive Poly (N-isopropylacrylamide)/Graphene Oxide Nanocomposite Hydrogels with Ultrahigh Tensibility. *ACS Appl. Mater. Interfaces* **2015**, *7*, 27289-27298.

(9) Yao, C.; Liu, Z.; Yang, C.; Wang, W.; Ju, X. J.; Xie, R.; Chu, L. Y. Poly (N-isopropylacrylamide)-Clay Nanocomposite Hydrogels with Responsive Bending Property as Temperature-Controlled Manipulators. *Adv. Funct. Mater.* **2015**, *25*, 2980-2991.

(10) Sershen, S. R.; Westcott, S. L.; Halas, N. J.; West, J. L. Temperature-Sensitive Polymer-Nanoshell Composites for Photothermally Modulated Drug Delivery. *J. Biomed. Mater. Res. A* **2000**, *51*, 293-298.

(11) Meng, H.; Xue, M.; Xia, T.; Zhao, Y. L.; Tamanoi, F.; Stoddart, J. F.; Zink, J. I.; Nel, A. E. Autonomous In Vitro Anticancer Drug Release from Mesoporous Silica Nanoparticles by PH-Sensitive Nanovalves. *J. Am. Chem. Soc.* **2010**, *132*, 12690-12697.

(12) Zhang, S. Y.; Bellinger, A. M.; Glettig, D. L.; Barman, R.; Lee, Y.-A. L.; Zhu, J.; Cleveland, C.; Montgomery, V. A.; Gu, L.; Nash, L. D. A PH-Responsive Supramolecular Polymer Gel as An Enteric Elastomer for Use in Gastric Devices. *Nat. Mater.* **2015**, *14*, 1065-1071.

(13) Nan, J. Y.; Chen, Y.; Li, R. T.; Wang, J. F.; Liu, M. H.; Wang, C. P.; Chu, F. X. Polymeric Hydrogel Nanocapsules: A Thermo and PH Dual-Responsive Carrier for Sustained Drug Release. *Nano-Micro Lett.* **2014**, *6*, 200-208.

(14) Zhang, X. B.; Pint, C. L.; Lee, M. H.; Schubert, B. E.; Jamshidi, A.; Takei, K.; Ko, H.; Gillies, A.; Bardhan, R.; Urban, J. J. Optically and Thermally responsive Programmable Materials Based on Carbon Nanotube-Hydrogel Polymer Composites. *Nano Lett.* **2011**, *11*, 3239-3244.

(15) Epstein-Barash, H.; Orbey, G.; Polat, B. E.; Ewoldt, R. H.; Feshitan, J.; Langer, R.; Borden, M. A.; Kohane, D. S. A Microcomposite Hydrogel for Repeated On-Demand Ultrasound-Triggered Drug Delivery. *Biomaterials* **2010**, *31*, 5208-5217.

(16) Hoare, T.; Santamaria, J.; Goya, G. F.; Irusta, S.; Lin, D.; Lau, S.; Padera, R.; Langer, R.; Kohane, D. S. A Magnetically Triggered Composite Membrane for On-Demand Drug Delivery. *Nano Lett.* **2009**, *9*, 3651-3657.

(17) Hoare, T.; Timko, B. P.; Santamaria, J.; Goya, G. F.; Irusta, S.; Lau, S.; Stefanescu, C. F.; Lin, D.; Langer, R.; Kohane, D. S. Magnetically Triggered Nanocomposite Membranes: A Versatile Platform for Triggered Drug Release. *Nano Lett.* **2011**, *11*, 1395-1400.

(18) Hauser, A. W.; Evans, A. A.; Na, J. H.; Hayward, R. C. Photothermally Reprogrammable Buckling of Nanocomposite Gel Sheets. *Angew. Chem., Int. Ed.* **2015**, *54*, 5434-5437.

(19) Cheng, Z.; Chai, R.; Ma, P.; Dai, Y.; Kang, X.; Lian, H.; Hou, Z.; Li, C.; Lin, J. Multiwalled Carbon Nanotubes and NaYF4: Yb3+/Er3+ Nanoparticle-Doped Bilayer Hydrogel for Concurrent Nir-Triggered Drug Release and Up-Conversion Luminescence Tagging. *Langmuir* **2013**, *29*, 9573-9580.

(20) Qu, Y.; Chu, B. Y.; Peng, J. R.; Liao, J. F.; Qi, T. T.; Shi, K.; Zhang, X. N.; Wei, Y. Q.; Qian, Z. Y. A Biodegradable Thermo-Responsive Hybrid Hydrogel: Therapeutic Applications in Preventing the Post-Operative Recurrence of Breast Cancer. *NPG Asia Mater.* **2015**, *7*, e207.

(21) Han, L.; Zhang, Y.; Lu, X.; Wang, K.; Wang, Z.; Zhang, H. Polydopamine Nanoparticles Modulating Stimuli-Responsive PNIPAM Hydrogels with Cell/tissue Adhesiveness. *ACS Appl. Mater. Interfaces* **2016**, *8*, 29088-29100.

(22) Luk, B. T.; Zhang, L. Current Advances in Polymer-Based Nanotheranostics for Cancer Treatment and Diagnosis. *ACS Appl. Mater. Interfaces* **2014**, *6*, 21859–21873.

(23) Huang, S.; Kannadorai, R. K.; Chen, Y.; Liu, Q.; Wang, M. F. A Narrow-Bandgap Benzobisthiadiazole Derivative with High Near-Infrared Photothermal Conversion Efficiency and Robust Photostability for Cancer Therapy. *Chem. Commun.* **2015**, *51*, 4223-4226.

(24) Lyu, Y.; Xie, C.; Chechetka, S. A.; Miyako, E.; Pu, K. Semiconducting Polymer Nanobioconjugates for Targeted Photothermal Activation of Neurons. *J. Am. Chem. Soc.* **2016**, *138*, 9049-9052.

(25) Pang, X. C.; Zhao, L.; Akinc, M.; Kim, J. K.; Lin, Z. Q. Novel Amphiphilic Multi-Arm, Star-Like Block Copolymers as Unimolecular Micelles. *Macromolecules* **2011**, *44*, 3746-3752.

(26) Pecher, J.; Mecking, S. Nanoparticles of Conjugated Polymers. *Chem. Rev.* **2010**, *110*, 6260-6279.

(27) Kamaly, N.; Xiao, Z.; Valencia, P. M.; Radovic-Moreno, A. F.; Farokhzad, O. C. Targeted Polymeric Therapeutic Nanoparticles: Design, Development and Clinical Translation. *Chem. Soc. Rev.* **2012**, *41*, 2971-3010.

(28) Sanghvi, A. B.; Miller, K. P.-H.; Belcher, A. M.; Schmidt, C. E. Biomaterials Functionalization Using a Novel Peptide that Selectively Binds to a Conducting Polymer. *Nat. Mater.* **2005**, *4*, 496-502.

(29) Geng, J.; Sun, C.; Liu, J.; Liao, L.; Yuan, Y.; Thakor, N.; Wang, J.; Liu, B. Biocompatible Conjugated Polymer Nanoparticles for Efficient Photothermal Tumor Therapy. *Small* **2015**, *11*, 1603-1610.

(30) Luk, B. T.; Zhang, L. Current Advances in Polymer-Based Nanotheranostics for Cancer Treatment and Diagnosis. *ACS Appl. Mater. Interfaces* **2014**, *6*, 21859-21873.

(31) Wu, C. F.; Chiu, D. T. Highly Fluorescent Semiconducting Polymer Dots for Biology and Medicine. *Angew. Chem. Int. Ed.* **2013**, *52*, 3086-3109.

(32) Zheng, T. Y.; Bott, S.; Huo, Q. Techniques for Accurate Sizing of Gold Nanoparticles Using Dynamic Light Scattering with Particular Application to Chemical and Biological Sensing Based on Aggregate Formation. *ACS Appl. Mater. Interfaces* **2016**, *8*, 21585-21594.

(33) Gorelikov, I.; Field, L. M.; Kumacheva, E. Hybrid Microgels Photoresponsive in the Near-Infrared Spectral Range. *J. Am. Chem. Soc.* **2004**, *126*, 15938-15939.

(34) Wu, G.; Mikhailovsky, A.; Khant, H. A.; Fu, C.; Chiu, W.; Zasadzinski, J. A. Remotely Triggered Liposome Release by Near-Infrared Light Absorption via Hollow Gold Nanoshells. *J. Am. Chem. Soc.* **2008**, *130*, 8175-8177.

(35) Hirano, A.; Tanaka, T.; Kataura, H. Thermodynamic Determination of The Metal/Semiconductor Separation of Carbon Nanotubes Using Hydrogels. *ACS Nano* **2012**, *6*, 10195-10205.

(36) Medintz, I. L.; Uyeda, H. T.; Goldman, E. R.; Mattoussi, H. Quantum Dot Bioconjugates For Imaging, Labelling and Sensing. *Nat. Mater.* **2005**, *4*, 435-446.

(37) Michalet, X.; Pinaud, F.; Bentolila, L.; Tsay, J.; Doose, S.; Li, J.; Sundaresan, G.; Wu, A.; Gambhir, S.; Weiss, S. Quantum Dots for Live Cells, In Vivo Imaging, and Diagnostics. *Science* **2005**, *307*, 538-544.

(38) Huang, S.; Upputuri, P. K.; Liu, H.; Pramanik, M.; Wang, M. F. A Dual-Functional Benzobisthiadiazole Derivative as an Effective Theranostic Agent for Near-Infrared Photoacoustic Imaging and Photothermal Therapy. *J. Mater. Chem. B* **2016**, *4*, 1696-1703.

(39) Lee, J.; Han, A.-R.; Kim, J.; Kim, Y.; Oh, J. H.; Yang, C. Solution-Processable Ambipolar Diketopyrrolopyrrole-Selenophene Polymer with Unprecedentedly High Hole and Electron Mobilities. *J. Am. Chem. Soc.* **2012**, *134*, 20713-20721.

(40) Yun, H. J.; Kang, S. J.; Xu, Y.; Kim, S. O.; Kim, Y. H.; Noh, Y. Y.; Kwon, S. K. Dramatic Inversion of Charge Polarity in Diketopyrrolopyrrole-Based Organic Field- Effect Transistors via a Simple Nitrile Group Substitution. *Adv. Mater.* **2014**, *26*, 7300-7307.

(41) Kang, I.; Yun, H. J.; Chung, D. S.; Kwon, S. K.; Kim, Y. H. Record High Hole Mobility in Polymer Semiconductors via Side-Chain Engineering. *J. Am.Chem. Soc.* **2013**, *135*, 14896-14899.

(42) Mohebbi, A. R.; Yuen, J.; Fan, J.; Munoz, C.; Shirazi, R. S.; Seifter, J.; Wudl, F. Emeraldicene as an Acceptor Moiety: Balanced-Mobility, Ambipolar, Organic Thin-Film Transistors. *Adv. Mater.* **2011**, *23*, 4644-4648.

(43) Wang, K.; Wang, M. F. Direct Arylation Polymerization: A Green, Streamlining Synthetic Approach to π-conjugated Polymers. *Curr. Org. Chem.* **2013**, *17*, 999-1012.

(44) Kowalski, S.; Allard, S.; Zilberberg, K.; Riedl, T.; Scherf, U. Direct Arylation Polycondensation as Simplified Alternative for the Synthesis of Conjugated (co) polymers. *Prog. Polym. Sci.* **2013**, *38*, 1805-1814.

(45) Facchetti, A.; Vaccaro, L.; Marrocchi, A. Semiconducting Polymers Prepared by Direct Arylation Polycondensation. *Angew. Chem. Int. Ed.* **2012**, *51*, 3520-3523.

(46) Huo, L.; Hou, J.; Chen, H.-Y.; Zhang, S.; Jiang, Y.; Chen, T. L.; Yang, Y. Bandgap and Molecular Level Control of the Low-Bandgap Polymers Based on 3, 6-dithiophen-2-yl-2, 5-dihydropyrrolo [3, 4-c] pyrrole-1, 4-dione Toward Highly Efficient Polymer Solar Cells. *Macromolecules* **2009**, *42*, 6564-6571.

(47) Li, W. w.; Roelofs, W. C.; Wienk, M. M.; Janssen, R. A. Enhancing the Photocurrent in Diketopyrrolopyrrole- based Polymer Solar Cells via Energy Level Control. *J. Am. Chem. Soc.* **2012**, *134*, 13787-13795.

(48) Pu, K. y.; Mei, J. G.; Jokerst, J. V.; Hong, G.; Antaris, A. L.; Chattopadhyay, N.; Shuhendler, A. J.; Kurosawa, T.; Zhou, Y.; Gambhir, S. S. Diketopyrrolopyrrole-Based Semiconducting Polymer Nanoparticles for In Vivo Photoacoustic Imaging. *Adv. Mater.* **2015**, *27*, 5184-5190.

(49) Liu, Y.; Ai, K.; Liu, J.; Deng, M.; He, Y.; Lu, L. Dopamine-Melanin Colloidal Nanospheres: An Efficient Near-Infrared Photothermal Therapeutic Agent for In Vivo Cancer Therapy. *Adv. Mater.* **2013**, *25*, 1353-1359.

(50) Roper, D. K.; Ahn, W.; Hoepfner, M. Microscale Heat Transfer Transduced by Surface Plasmon Resonant Gold Nanoparticles. *J. Phys. Chem. C* **2007**, *111*, 3636-3641.

(51) Xu, Z. G.; Liu, S. Y.; Kang, Y. J.; Wang, M. F. Glutathione and PH-Responsive Nonporous Silica Prodrug Nanoparticles For Controlled Release and Cancer Therapy. *Nanoscale* **2015**, *7*, 5859-5868.

(52) Wang, X. C.; Wang, M. F. Synthesis of Donor-Acceptor Conjugated Polymers Based on Benzo [1, 2-b: 4, 5-b′] Dithiophene and 2, 1, 3- benzothiadiazole via Direct Arylation Polycondensation: Towards Efficient C-H Activation in Nonpolar Solvents. *Polym. Chem.* **2014**, *5*, 5784-5792.

(53) Wang, X. C.; Wang, K.; Wang, M. F. Synthesis of Conjugated Polymers via an Exclusive Direct-Arylation Coupling Reaction: A Facile and Straightforward Way to Synthesize Thiophene-Flanked Benzothiadiazole Derivatives and Their Copolymers. *Polym. Chem.* **2015**, *6*, 1846-1855.

(54) Wang, K.; Wang, G. J.; Wang, M. F. Balanced Ambipolar Poly (diketopyrrolopyrrole-alt-tetrafluorobenzene) Semiconducting Polymers Synthesized via Direct Arylation Polymerization. *Macromol. Rapid Comm.* **2015**, *36*, 2162-2170.

(55) Shao, J. J.; Wang, G. J.; Wang, K.; Yang, C. J.; Wang, M. F. Direct Arylation Polycondensation for Efficient Synthesis of Narrow-Bandgap Alternating D-A copolymers Consisting of Naphthalene Diimide as an Acceptor. *Polym. Chem.* **2015**, *6*, 6836-6844.

(56) Huang, J.; Wang, K.; Gupta, S.; Wang, G. J.; Yang, C. J.; Mushrif, S. H.; Wang, M. F. Thienoisoindigo-Based Small Molecules and Narrow Bandgap Polymers Synthesized via C-H Direct Arylation Coupling. *J. Polym. Sci. Pol. Chem.* **2016**.

(57) Bohra, H.; Shao, J. J.; Huang, S.; Wang, M. F. Facile Synthesis of Naphthodithiophenediimide Based Small Molecules and Polymers via Direct Arylation Coupling. *Tetrahedron Lett.* **2016**, *57*, 1497-1501.

(58) Efrem, A.; Wang, K.; Amaniampong, P. N.; Yang, C. J.; Gupta, S.; Bohra, H.; Mushrif, S. H.; Wang, M. F. Direct Arylation Polymerization Towards Narrow Bandgap Conjugated Microporous Polymers with Hierarchical Porosity. *Polym. Chem.* **2016**, *7*, 4862-4866.

(59) Bohra, H.; Tan, S. Y.; Shao, J. J.; Yang, C. J.; Efrem, A.; Zhao, Y. L.; Wang, M. F. Narrow Bandgap Thienothiadiazole-Based Conjugated Porous Polymers: From Facile Direct Arylation Polymerization to Tunable Porosities and Optoelectronic Properties. *Polym. Chem.* **2016**, *7*, 6413-6421.

(60) Pouliot, J.-R. m.; Grenier, F. o.; Blaskovits, J. T.; Beaupré, S.; Leclerc, M. Direct (Hetero) Arylation Polymerization: Simplicity for Conjugated Polymer Synthesis. *Chem. Rev.* **2016**, *116*, 114225-1142.

(61) Lyu, Y.; Xie, C.; Chechetka, S. A.; Miyako, E.; Pu, K. Y. Semiconducting Polymer Nanobioconjugates for Targeted Photothermal Activation of Neurons. *J. Am. Chem. Soc.* **2016**, *138*, 9049-9052.

(62) Halperin, A.; Kröger, M.; Winnik, F. M. Poly (N-isopropylacrylamide) Phase Diagrams: Fifty Years of Research. *Angew. Chem., Int. Ed.* **2015**, *54*, 15342-15367.

Table of contents